

Magnetic properties and magnetoresistance in small iron oxide cluster assemblies

D. L. Peng,^{a)} T. Asai, N. Nozawa, T. Hihara, and K. Sumiyama

Department of Materials Science and Engineering, Nagoya Institute of Technology, Nagoya 466-8555, Japan

(Received 15 July 2002; accepted 21 October 2002)

We report the magnetic properties and magnetoresistance (MR) in small iron oxide ($\text{Fe}_{3-x}\text{O}_4$ and Fe_3O_4) cluster assemblies. Half-metallic Fe_3O_4 cluster assembly with grain size of 10–15 nm is shown to exhibit a MR value of about 8% at $T=30$ K and a peak around the Verwey transition temperature $T_v=115$ K which is a little lower than the T_v value (~ 120 K) of single crystal specimens. Even at $T=5$ K, the magnetization is not saturated in fields up to 50 kOe. The MR behaviors of a $\text{Fe}_{3-x}\text{O}_4$ -coated iron cluster assembly and a sample which was prepared by embedding the $\text{Fe}_{3-x}\text{O}_4$ -coated iron clusters into a MgO matrix are also studied for comparison. The MR value of the latter is over one time larger than that of the former and is also larger than those of the Fe_3O_4 cluster assembly at various temperatures. It suggests that the barrier layer is important for enhancing the MR effect at high temperatures. © 2002 American Institute of Physics. [DOI: 10.1063/1.1528725]

There has been a growing interest in the tunneling magnetoresistance (TMR) effect in materials due to their potential applications for magnetoresistive devices.^{1,2} TMR arises from a spin-dependent tunneling effect. Electron tunneling between two ferromagnetic electrodes through an insulator (I) layer depends on the relative orientation of the magnetizations of the electrodes. When the relative orientation of the magnetizations is changed by applying a magnetic field, a marked negative TMR is expected. In a magnetic granular system, the fundamental quantity which determines the TMR ratio is the spin polarization (P) of electrons in the ferromagnetic metal (FM) granules. $P=0$ corresponds to paramagnetic metals and $P=1$ to half metals in which only one spin subband makes a contribution to the tunneling conduction of electrons. Since the TMR ratio is proportional to P^2 either in FM/I/FM junctions or in magnetic granular systems, it is a straightforward way of enhancing the TMR to use the high spin polarization or half-metallic FMs in the tunnel-type nanostructures.

Half metallicity is known for CrO_2 ,^{3–5} Fe_3O_4 ,^{6,7} and $\text{La}_{0.7}\text{Sr}_{0.3}\text{MnO}_3$ (LSMO).^{8,9} Large TMR effects have already been observed at low temperature for CrO_2 polycrystalline,^{3,5} $\text{CrO}_2\text{-Cr}_2\text{O}_3$ granular systems⁴ and $\text{La}_{2/3}\text{Sr}_{1/3}\text{MnO}_3$ polycrystalline,¹⁰ as well as their FM/I/FM-type junctions.^{9,11} Since TMR devices requires a high Curie temperature (T_c), Fe_3O_4 with high Curie temperature ($T_c=850$ K) is attractive in comparison to LSMO ($T_c=360$ K) and CrO_2 ($T_c=395$ K). Indeed, TMR effects are not large in Fe_3O_4 polycrystalline thin film and powder compact,¹² but so marked in epitaxial Fe_3O_4 films¹³ and tunnel junctions with a combination of Co and Fe_3O_4 electrodes⁷ as well as LSMO and Fe_3O_4 electrodes.¹⁴

In this letter, we report the magnetic properties and MR effect in small iron oxide ($\text{Fe}_{3-x}\text{O}_4$ and Fe_3O_4) cluster assemblies. These samples were first prepared by the plasma-

gas-condensation (PGC)-type cluster beam deposition apparatus.¹⁵ The apparatus is composed of the three main parts: a sputtering chamber, a cluster growth room, and a deposition chamber. Sample 1 is a highly surface-oxidized Fe cluster assembly (with an initial Fe cluster mean size $d=13$ nm), which was prepared by the introduction of oxygen gas through a nozzle into the deposition chamber to form iron oxide shells covering the Fe clusters before depositing on the substrate. This process ensures that all Fe clusters are highly oxidized before the cluster assemblies are formed. High resolution transmission electron microscopy (TEM) observation (not shown here) and electron diffraction (ED) pattern [Fig. 1(a)] show that the Fe cores with $d=9$ nm were covered with $\text{Fe}_{3-x}\text{O}_4$ ($0 \leq x \leq 0.33$) shells composed of very small crystallites with the size of $d=2-3$ nm. Sample 2 was obtained by annealing sample 1 at $T=573$ K for 2 h in a gas pressure of about 2×10^{-6} Torr. Figure 1(b) shows that sample 2 is composed of only Fe_3O_4 grains whose sizes ($d=10-15$ nm) are observed by TEM. Sample 3 was prepared by combination of an embedding method. $\text{Fe}_{3-x}\text{O}_4$ -coated Fe clusters (with the same condition as sample 1) was em-

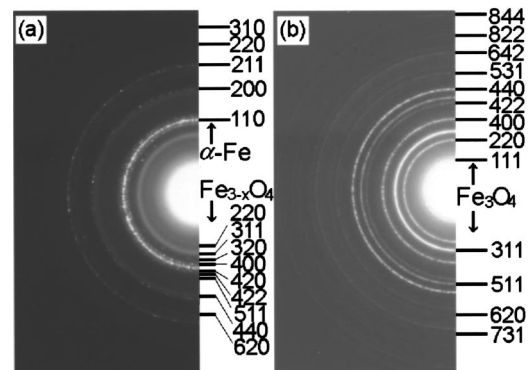


FIG. 1. Electron diffraction patterns for highly surface-oxidized Fe cluster assembly (sample 1) and only Fe_3O_4 grain assembly (sample 2) obtained by annealing of the No. 1 sample at $T=573$ K for 2 h.

^{a)}Electronic mail: pengdl@mse.nitech.ac.jp

TABLE I. Characteristics of the samples used in this work. All data are at $T=300$ K.

Sample No.	Oxide grain size d (nm)	Resistivity ρ ($\mu\Omega$ cm)	$[\rho_{H=0}-\rho_{H=50\text{ kOe}}]/\rho_{H=50\text{ kOe}}$ MR (%)	Thickness t_c (nm)
1	2-3	8.40×10^4	1.20	480
2	10-15	1.73×10^4	1.91	410
3	2-3	7.47×10^6	2.78	80

bedded in a MgO matrix, where they are separated by the MgO barriers with nonuniform thickness. The details of these three samples are listed in Table I. The effective film thickness of deposited clusters, t_e , was estimated using a quartz crystal thickness monitor, which measures the weight of the deposited clusters. Magnetic measurement was performed using a superconducting quantum interference device magnetometer between 5 and 300 K in magnetic fields up to 50 kOe. Electrical resistivity was measured using a conventional dc four-probe method, and MR measurement was made in fields applied parallel to the electrical current direction.

Figure 2 shows hysteresis loops measured in a field range of -50 – 50 kOe for the samples 1 and 2 at 5 K. For sample 1 [Fig. 2(a)], the hysteresis loop exhibits a two-step saturation behavior. The rapidly saturated part corresponds to ferromagnetic Fe cores, while the slowly saturated part is to ferrimagnetic $\text{Fe}_{3-x}\text{O}_4$ shell crystallites with $d=2$ – 3 nm. The large coercivity value ($H_c = 1150$ Oe) is ascribed to both an intrinsic property of ferromagnetic single-domain Fe cores and an extrinsic property related to the exchange anisotropy.¹⁶ For sample 2 [Fig. 2(b)], the hysteresis loop is of a different shape in comparison with sample 1. The coercivity also decreases to 770 Oe. For these two samples, however, there is the same feature: the magnetization does not saturate up to $H=50$ kOe (see the inset of Fig. 2) and $M_{H=10\text{ kOe}}$ is about 0.9 time of $M_{H=50\text{ kOe}}$ at $T=5$ K. This is attributable to a surface spin disorder state (spin-glass-like

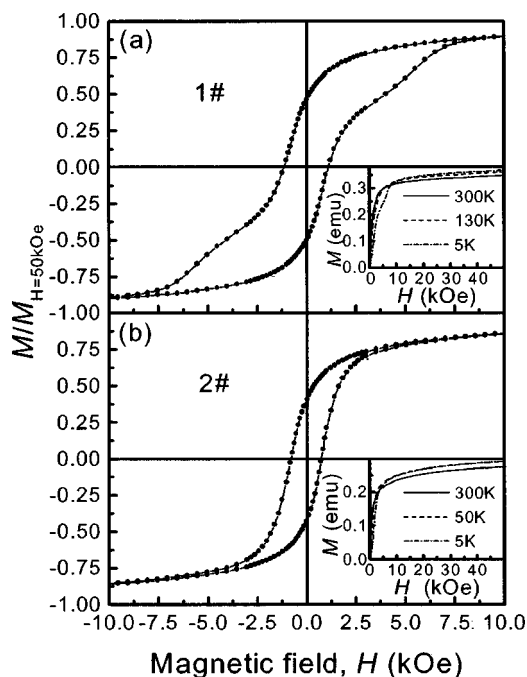


FIG. 2. Hysteresis loops of the sample Nos. 1 and 2 at 5 K. The inset shows the initial magnetization curves at different temperatures.

state) of nanoscale ferrimagnetic Fe oxide particle system.¹⁷

Figure 3(a) shows the temperature (T) dependence of the electrical resistivity, $\rho(T)$, for the three samples. At room temperature (RT), the ρ value for sample 1 is $8.4 \times 10^4 \mu\Omega$ cm. This value is 2.4 times as large as that ($3.5 \times 10^4 \mu\Omega$ cm) of polycrystalline film,¹² and 8 times as large as that ($\sim 1 \times 10^4 \mu\Omega$ cm) for the epitaxial Fe_3O_4 film (660 nm).¹³ It monotonically increases with decreasing temperature. For sample 2, the ρ value at RT is $1.7 \times 10^4 \mu\Omega$ cm, which is close to but still larger than that for the epitaxial Fe_3O_4 film.¹³ This indicates the dominant contribution of grain-boundary resistance. As T decreases, the ρ value gradually increases like a semiconductor, while it abruptly increases at around 115 K, corresponding to the Verwey transition temperature (T_v). This value is a little lower than the T_v value (~ 120 K) for a Fe_3O_4 bulk sample but is consistent with the measured result of the MR [Fig. 3(b)]. This suggests that the annealing process makes the sample more stoichiometric.

Figure 3(b) shows the temperature (T) dependence of high-field MR ratio, $[\rho_{H=0}-\rho_{H=50\text{ kOe}}]/\rho_{H=50\text{ kOe}}$, for the three samples. With decreasing T , the MR ratio monotonically increases for sample 1, while it increases slightly in the range of $130 < T < 300$ K, and exhibits a peak around $T_v = 115$ K, and then increases markedly with decreasing T be-

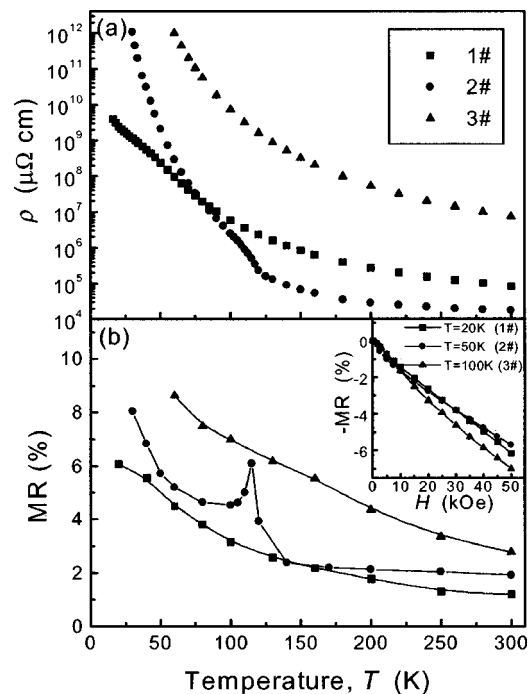


FIG. 3. Temperature dependence of (a) electrical resistivity ρ at zero magnetic field and (b) MR ratio, $[\rho_{H=0}-\rho_{H=50\text{ kOe}}]/\rho_{H=50\text{ kOe}}$, for sample, Nos. 1, 2, and 3. The inset shows magnetic field dependence of the MR ratio at low temperatures.

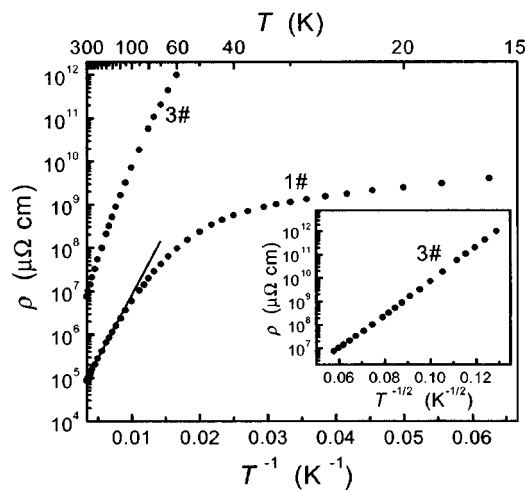


FIG. 4. Logarithmic resistivity, $\log \rho$, as a function of T^{-1} for sample Nos. 1 and 3. Solid lines show the $\log \rho$ vs T^{-1} fitting between 140 and 300 K. The inset shows the logarithmic resistivity, $\log \rho$, as a function of $T^{-1/2}$ for sample No. 3.

low 80 K for sample 2, i.e., from 4.6% at 80 K to 8.0% at 30 K. On the other hand, sample 3 exhibits an enhanced MR effect, i.e., its MR value is twice as large as that of sample 1, being due to the increase of the intergrain transport through the MgO barriers. As shown in the inset of Fig. 3, moreover, the magnetic field dependence of the MR for the three samples exhibit no saturation tendency. Clearly, this feature disagrees with the magnetization curves (the inset of Fig. 2) which are of a saturation tendency, in spite of gradual increase of magnetization for $H > 10$ kOe. In nanogranular alloys containing uncorrelated magnetic scatters such as superparamagnetic magnetic particles,¹⁸ the MR should be proportional to M^2 . In addition, as seen in Fig. 3(b), the MR values observed for all samples are much smaller than the expected high MR values for the half-metallic materials. Since magnetotunneling is an interface effect, the high-field nonsaturation behavior and the lower MR values for the present systems may result from spin disorder at Fe_3O_4 grain surface.¹⁹ Such a surface spin disorder has been experimentally discussed in ferrite nanoparticles²⁰ and small Fe oxide grains.¹⁷ The antiferromagnetic superexchange interaction is disrupted at the surface of the ferrimagnetic oxide crystallites because of missing oxygen ions or the presence of other impurity molecules. Such broken exchange bonds between surface spins lead to surface spin disorder.

Finally, it is worth further discussion on the temperature dependence of the resistivity for samples 1 and 3. Figure 4 shows $\log \rho$ vs $1/T$ curves for the samples 1 and 3 and $\log \rho$ vs $1/T^{1/2}$ for 3 sample (inset). A linear dependence of $\log \rho$ vs $1/T$ is observed in the range of $130 < T < 300$ K for sample 1. This behavior is ascribed to fluctuation-induced tunneling conduction mechanism in disordered materials,²¹ in which the thermally activated voltage fluctuations across tunneling barriers play an important role in determining the temperature dependence of the conductivity. At high temperature, the tunneling conductivity displays thermally activated characteristics [$\rho \propto \exp(T_1/T)$]. As seen in the inset, on the other hand, the MgO barriers with nonuniform thickness gives rise to $\log \rho \propto 1/T^{1/2}$ dependence over a wide temperature range

($60 < T < 300$ K) for sample 3. Similar behavior has been reported for well-defined Co clusters embedded in inert-gas solid matrices.²² According to Sheng *et al.*,²³ the $\rho \propto \exp(T_0/T)^{1/2}$ dependence has been derived from the assumption that the separation s between grains (namely the tunnel-barrier thickness) is proportional to the grain size d in granular materials. In our case, however, the size ($d = 2-3$ nm) of the oxide shell crystallites is not correlated to the MgO barrier thickness. Therefore, the $\log \rho \propto 1/T^{1/2}$ temperature dependence in our sample 3 is ascribable to another hopping model in which the barrier thickness is a random variable uncorrelated with the activation energy (namely, size d) which is dominated by the intragrain level splitting.^{24,25}

This work has been supported by Core Research for Evolutional Science and Technology (CREST) of Japan Science and Technology Corporation (JST). One of the authors (D.L.P.) appreciates the financial support from Japan Society for the Promotion of Science (JSPS).

- ¹J. J. Sun, K. Shimazawa, N. Kasahara, K. Sato, S. Saruki, T. Kagami, O. Redon, S. Araki, H. Morita, and M. Matsuzaki, *Appl. Phys. Lett.* **76**, 2424 (2000).
- ²P. Chen, D. Y. Xing, Y. W. Du, J. M. Zhu, and D. Feng, *Phys. Rev. Lett.* **87**, 107202 (2001).
- ³H. Y. Hwang and S.-W. Cheong, *Science* **278**, 1607 (1997).
- ⁴J. M. D. Coey, A. E. Berkowitz, L. Balcells, and F. F. Putris, *Phys. Rev. Lett.* **80**, 3815 (1998).
- ⁵S. Sundar Manoharan, D. Elefant, G. Reiss, and J. B. Goodenough, *Appl. Phys. Lett.* **72**, 984 (1998).
- ⁶Z. Zhang and S. Satpathy, *Phys. Rev. B* **44**, 13319 (1991).
- ⁷P. Senor, A. Fert, J.-L. Aurice, F. Montaigne, F. Petroff, and A. Vaures, *Appl. Phys. Lett.* **74**, 4017 (1999).
- ⁸J. H. Park, E. Vescovo, H. J. Kim, C. Kwon, R. Ramesh, and T. Venkatesan, *Nature (London)* **392**, 794 (1998).
- ⁹J. M. De Teresa, A. Barthélémy, A. Fert, J. P. Contour, R. Lyonnet, F. Montaigne, P. Senor, and A. Vaurès, *Phys. Rev. Lett.* **82**, 4288 (1999).
- ¹⁰H. Y. Hwang, S. W. Cheong, N. P. Ong, and B. Batlogg, *Phys. Rev. Lett.* **77**, 2041 (1996).
- ¹¹J. O'Donnell, A. E. Andrus, S. Oh, E. V. Colla, and J. N. Eckstein, *Appl. Phys. Lett.* **76**, 1914 (2000).
- ¹²J. M. D. Coey, A. E. Berkowitz, L. Balcells, F. F. Putris, and F. T. Parker, *Appl. Phys. Lett.* **72**, 734 (1998).
- ¹³G. Q. Gong, A. Gupta, G. Xiao, W. Qian, and V. P. Dravid, *Phys. Rev. B* **56**, 5096 (1997).
- ¹⁴K. Ghosh, S. B. Ogale, S. P. Pai, M. Robson, E. Li, I. Jin, Z.-W. Dong, R. L. Greene, R. Ramesh, T. Venkatesan, and M. Johnson, *Appl. Phys. Lett.* **73**, 689 (1998).
- ¹⁵S. Yamamuro, K. Sumiyama, and K. Suzuki, *J. Appl. Phys.* **85**, 483 (1999).
- ¹⁶W. H. Meiklejohn and C. P. Bean, *Phys. Rev.* **102**, 1413 (1956); **105**, 904 (1957).
- ¹⁷L. Del Bianco, A. Hernando, M. Multigner, C. Prados, J. C. Sanchez-Lopez, A. Fernandez, C. F. Conde, and A. Conde, *J. Appl. Phys.* **84**, 2189 (1998).
- ¹⁸C. L. Chien, J. Q. Xiao, and J. S. Jiang, *J. Appl. Phys.* **73**, 5309 (1993).
- ¹⁹L. Savini, E. Bonetti, L. Del Bianco, L. Pasquini, S. Signoretti, P. Allia, M. Coisson, J. Moya, V. Selvaggini, P. Tiberto, and F. Vinai, *J. Appl. Phys.* **91**, 8593 (2002).
- ²⁰R. H. Kodama, A. E. Berkowitz, E. J. McNiff, and S. Foner, *Phys. Rev. Lett.* **77**, 394 (1996).
- ²¹P. Sheng, *Phys. Rev. B* **21**, 2180 (1980).
- ²²M. Holdenried, B. Hackenbroich, and H. Micklitz, *J. Magn. Magn. Mater.* **231**, L13 (2001).
- ²³P. Sheng, B. Abeles, and Y. Arie, *Phys. Rev. Lett.* **31**, 44 (1973).
- ²⁴E. Simanek, *Solid State Commun.* **40**, 1021 (1981).
- ²⁵G. F. Hohl, S. D. Baranovskii, J. A. Becker, F. Hensel, S. A. Quaiser, and M. T. Reetz, *J. Appl. Phys.* **78**, 7130 (1995).